Optimizing Zinc Recovery in Sulfide Mineral Flotation for Geometallurgical Characterization

Julio Berrocal-Majerhua[ID], Vidal S. Aramburú-Rojas[ID], Jorge A. Ortiz-Barreto[ID], Leonel A. Alvarez-Llanos[ID], Jack B. Moran-Mendoza[ID], Luis M. Soto-Juscamayta*[ID]

Faculty of Geological, Mining, Metallurgical and Geographic Engineering, Universidad Nacional Mayor de San Marcos, Lima 0711, Peru

Corresponding Author Email: luis.soto.14@unmsm.edu.pe

ABSTRACT

This study aims to optimize zinc recovery from sulfide mineral flotation in the province of Oyón, Peru, by integrating detailed mineralogical characterization with a rigorous experimental design. Optical microscopy and TIMA electron microscopy identified marmatitic sphalerites with 17.24% distribution and 99.51% free species, along with gangue minerals such as epidote, garnet, and quartz. A three-factor experimental design evaluated $ZnSO_4$, NaCN dosage, and flotation pH to minimize zinc displacement during Pb-Cu bulk flotation, achieving a minimum Zn displacement of 5.14% with a 1.24% grade. Zn flotation tests optimized $CuSO_4$ and Xanthate Z-11 dosages, resulting in a zinc recovery of 97.61% and a concentrate grade of 48.06%. This comprehensive approach demonstrates significant improvements in zinc recovery and offers a replicable methodology for other mining regions with complex mineralogies, contributing to more sustainable and efficient mining practices.

1. INTRODUCTION

Mineral recovery in the mining industry is a global challenge [1, 2], especially in the extraction of metals such as zinc, which is crucial for various industrial applications from galvanization to alloy manufacturing. According to the United States Geological Survey, global zinc production in 2021 was approximately 13 million tons, with China, Peru and Australia being the main producers [3, 4]. The growing demand for zinc, driven by its use in corrosion protection and the automotive industry, has intensified the need to optimize recovery processes to ensure a continuous and efficient supply [5-7]. This demand is expected to continue to increase due to the growth of the electric vehicle industry, where zinc is an essential component in batteries and other electronic devices [7].

Zinc recovery methods have evolved significantly in recent decades, but still face significant technical challenges [8-10]. Traditional flotation methods have been complemented by advanced biohydrometallurgy and leaching techniques; however, the efficiency of these methods can be affected by variability in the mineralogy of the deposits and the specific conditions of each mine [11, 12]. Although zinc recovery by flotation has been widely studied, previous research has not comprehensively addressed the complex interactions between different minerals present in geometallurgically complex deposits such as those in the Oyón Province. Studies such as those by Jia et al. [7] have highlighted the influence of sulfide species in inhibiting selective zinc flotation, but have not offered solutions that address mineralogical variability. This study builds on this background and seeks to close these gaps by implementing advanced mineralogical characterization techniques and a robust experimental design that optimizes zinc recovery under specific local conditions.

For example, a study conducted by Chandra and Gerson [13] highlighted how zinc activation in the presence of pyrite and other sulfide minerals can inhibit selective zinc flotation due to complex galvanic interactions that are not always predictable and require precise control of the chemical environment.

Peru is the second largest producer of zinc in the world, with an annual production exceeding 1.4 million tons, contributing significantly to the country's economy [14-16]. Zinc mining in Peru is a vital industry, with regions such as Ancash, Pasco and Lima playing crucial roles in the extraction of this metal [17]. However, the industry faces significant challenges related to the efficiency of recovery processes and environmental sustainability. The sulfide mineral deposits in these regions present a geological complexity that makes effective zinc recovery difficult, underlining the need for advanced research to improve processing techniques [17]. In particular, the presence of gangue minerals such as pyrite, which compete with sphalerite (main zinc mineral) for flotation reagents, represents a significant challenge for concentrator plants.

In the province of Oyón, located in the Lima region, the extraction of sulfide minerals is a key economic activity. The deposits in Oyón contain valuable species such as sphalerite, marmatite, galena, and traces of gold and electrum. However, zinc recovery in these deposits faces obstacles due to

mineralogical complexity and the presence of gangue species that interfere with the flotation process. Previous studies have shown that variability in mineralogical composition and suboptimal operating conditions can lead to suboptimal zinc recovery, negatively affecting the profitability and sustainability of mining operations [18]. Furthermore, the mountainous geography and extreme climatic conditions of the region can influence the effectiveness of processing techniques, making it essential to develop strategies adapted to these local conditions.

Despite advances in flotation techniques and mineralogical characterization, significant knowledge gaps remain that limit the efficiency of zinc recovery. One of the main challenges is the selective activation of sphalerite in the presence of pyrite and other sulfide minerals. Galvanic interaction between these minerals can inhibit selective zinc flotation, a problem that has been documented but not fully resolved [13]. Variability in mineralogical composition, particularly the presence of marmatite, a high-iron variant of sphalerite, can further complicate the flotation process due to their different surface properties and chemical reactivity.

Furthermore, accurate dosing of reagents such as $ZnSO_4$ and NaCN remains an area with room for improvement, as incorrect dosing can result in significant zinc losses and increased operating costs [19]. Optimization of these reagents is critical to maximizing zinc recovery and minimizing economic losses. Other studies have shown that flotation pulp pH is a critical factor affecting zinc recovery. However, the interaction of multiple operational variables and their combined impact on process efficiency has not been fully explored. This study addresses these knowledge gaps through a comprehensive approach that combines advanced mineralogical characterization techniques and rigorous experimental design to optimize flotation conditions [8].

Regarding this topic, there is little research that has comprehensively addressed the optimization of zinc recovery in sulfide minerals, which makes it a particularly relevant and interesting field of study. Although there are some previous studies that have explored various methodologies and techniques to improve zinc recovery, there are still important gaps in knowledge and areas with considerable potential for improvement.

According to the study by Wu et al. [20] aimed to optimize zinc recovery in the flotation of sulfide minerals by removing surface oxidation products, which reduce mineral hydrophobicity and hinder selective collector adsorption. To achieve this, mechanical (sonication and quartz attrition) and chemical (pH adjustment and use of complexing agents) methods were applied on various sulfide minerals. The effectiveness of these treatments was evaluated by correlating the amount of oxidation products removed with flotation results. "Cleaning" methods proved to be effective and selective, improving mineral hydrophobicity and collector adsorption, resulting in increased flotation efficiency. However, this study does not address zinc recovery optimization under complex geometallurgical conditions such as those at Oyón, Peru. This investigation will integrate advanced mineralogical characterization with a robust experimental design to optimize flotation conditions and maximize zinc recovery, addressing the mineralogical variability and specific conditions of the Oyón deposits.

On the other hand, there is the research carried out by Clarke et al. [21], the objective of this research was to optimize zinc recovery from sulfide ores by removing toxic heavy metals using potassium permanganate ($KMnO_4$). Using Aspen Plus software and the Taguchi method, a new configuration was evaluated where $KMnO_4$ is produced from cobalt purification sludge with MnO_2, and H_2SO_4 is obtained from sulfur compounds released during ore leaching. The Taguchi experimental design determined optimal conditions, which were used for simulation and sensitivity analysis of the process. These conditions included a H_2SO_4 concentration of 70 g/L, temperature of 90°C, stirring speed of 200 rpm, reaction time of 1.5 hours, particle size of 500 μm, solid-liquid ratio of 1:2, 40% additive by weight and oxygen pressure of 1.5 MPa. The results showed that the conversion of sulfide gases to H_2SO_4, $KMnO_4$ recovery, and toxic heavy metal removal reached 98%, 91%, and 99% respectively. However, their research does not address specific optimization for zinc recovery under the complex geometallurgical conditions of Oyón, Peru, which will be the focus of this research.

Likewise, there is a study carried out by Dominy et al. [22], where the objective of this investigation was to optimize zinc recovery in sulfide minerals by applying advanced oxidation processes (AOP) based on metal sulfides, known for their catalytic performance and stability. Aspen Plus software and the Taguchi method were used to evaluate a new configuration that uses potassium permanganate ($KMnO_4$) obtained from cobalt purification sludge and sulfuric acid (H_2SO_4) generated from sulfur gases released in leaching. Optimal operating conditions were established using the Taguchi experimental design and simulations and sensitivity analyses were performed. The results showed that under optimized conditions (70 g/L H_2SO_4, 90°C, 200 rpm, 1.5 hours, 500 μm particle size, 1:2 solid-liquid ratio, 40% additive by weight, and 1.5 MPa oxygen pressure), the conversion of sulfide gases to H_2SO_4, $KMnO_4$ recovery, and toxic heavy metal removal were 98%, 91%, and 99% respectively. However, this research does not address the specific integration of metal sulfide-based AOPs for zinc recovery in complex geometallurgical contexts, which will be the main focus of my research, seeking to improve the efficiency and sustainability of zinc recovery in Oyón, Peru.

The main objective of this study is to optimize zinc recovery from sulfide mineral deposits in the province of Oyón by implementing an experimental design that evaluates reagent dosage and pH of the flotation pulp. Using advanced optical and electron microscopy techniques, a detailed characterization of the mineral species present will be performed, allowing for the design of more efficient and sustainable processing strategies. This approach not only considers the individual properties of the minerals, but also their complex interactions and how this affect flotation efficiency.

Compared to previous research, this study not only focuses on the optimization of individual variables, but also considers the complex interactions between different operational factors. In addition, advanced statistical analysis techniques will be implemented to identify optimal flotation conditions, thereby improving zinc recovery and concentrate quality. This comprehensive approach not only optimizes the metallurgical process, but also contributes to the socio-economic development of the mining communities involved, promoting sustainable and efficient practices.

The relevance of this study lies in its potential to significantly improve the efficiency and sustainability of zinc recovery in the province of Oyón. By addressing existing knowledge gaps and applying a comprehensive optimization

approach, this research will not only benefit the local mining industry, but will also offer a replicable model for other regions with similar deposits. The results of this study will contribute to the development of more efficient and sustainable mining practices, supporting the Peruvian economy and protecting the environment.

This study differs from previous work by integrating a detailed analysis of the geometallurgical characterization with a robust experimental design that considers the interactions between multiple operational variables. Research such as that of Chen et al. [18], they have highlighted the importance of mineralogical characterization, but have not fully addressed how these characteristics can be integrated into a flotation optimization model. This study also considers long-term sustainability, assessing not only zinc recovery but also the environmental impact and economic viability of the proposed practices.

Unlike previous research, which has explored zinc sulfide mineral flotation more generally, this study is distinguished by its comprehensive focus on optimization under complex geometallurgical conditions, particularly in deposits in the Oyón Province. The integration of advanced optical microscopy and TIMA electron microscopy, combined with a multifactorial experimental design, represents a novel contribution to the field. Furthermore, the use of predictive modeling and statistical optimization allows for greater precision in the control of operational variables, significantly improving the efficiency and sustainability of zinc recovery.

2. MATERIALS AND METHODS

Optimizing zinc recovery in the flotation process of sulfide minerals in the Oyón Province, Peru, is crucial due to the geological complexity and economic importance of these deposits. Detailed mineral characterization and optimization of flotation conditions are critical to maximize zinc recovery and improve process efficiency. To achieve this, advanced mineralogical characterization techniques and rigorous experimental designs will be implemented to accurately replicate the study. The procedures and rationale for each stage of the study are described in detail below.

2.1 Mechanical preparation of the head ore

2.1.1 Sampling and size reduction
The first step in optimizing the flotation process is proper preparation of the head ore. The collected ore was reduced to a particle size of 100% -10 mesh using a "5×6" laboratory jaw crusher and a 21.5 cm cone crusher. This size reduction process is essential because it allows the mineral particles to be released from the gangue, thus improving efficiency in subsequent processing stages. Size reduction facilitates the exposure of valuable minerals, allowing their effective separation. The Bond equation for specific comminution energy is used to estimate the energy required for size reduction:

$$E = 10 W_i \left(\frac{1}{\sqrt{P_{80}}} - \frac{1}{\sqrt{F_{80}}} \right) \qquad (1)$$

where, E is the specific energy (kWh/ton), W_i is the Bond work index (kWh/ton), P_{80} is the particle size in the product (μm) and F_{80} is the particle size in the feed (μm) [5].

The crushed ore was then quartered to obtain a representative sample, which is crucial to avoid bias and ensure that the analyses are accurate and reproducible [18].

2.1.2 Optical and electron microscopy
For a detailed mineralogical characterization, a representative sample of 1000 g of ore was taken from the head, which was reduced in size in a laboratory ball mill with 14 kg of grinding charge and 500 ml of H_2O, reaching a particle size of 70.53% -200 mesh in 10 minutes of grinding. Additional size reduction is necessary to ensure that the particles are sufficiently liberated for accurate characterization. The ground sample was dried in an oven at 120°C for 2 hours. A subsample of approximately 20 g was mixed with epoxy resin to prepare a briquette, which after being properly polished, was observed by polarizing light optical microscopy. This method allows the identification of the mineral species present and their textures, but does not provide complete information on the composition of the gangues. For this reason, a ground mineral sample was sent to an electron microscopy laboratory to determine the composition of the gangues with greater precision [23]. The combination of these techniques provides a comprehensive mineralogical characterization, essential for designing efficient flotation processes [8].

2.1.3 Chemical analysis
To determine the ore grades of the minerals of interest, a representative sample of the head ore was sent to a laboratory. The grades of Pb, Cu and Zn were determined by the wet method, while those of Au and Ag were analyzed by the dry method. Chemical analysis is essential to know the elemental composition of the mineral, which guides the selection and adjustment of reagents in the flotation process. This analysis provides the necessary data to evaluate the economic viability of the deposit and design appropriate processing strategies [2, 22].

The chemical analysis was carried out using inductively coupled plasma optical emission spectrometry (ICP-OES) for Pb, Cu, and Zn grades, while fire assay was used for Au and Ag content. The equipment used for the ICP analysis was a PerkinElmer Optima 8000, and the results were validated with certified reference materials to ensure accuracy. The detection limits for each element were set at 0.01% for Pb, Cu, and Zn, and 0.1 g/t for Au and Ag.

2.2 Standard bulk flotation of Pb-Cu

2.2.1 Exploratory flotation test
An exploratory flotation test was performed to separate Pb and Cu minerals, depressing Zn minerals in a first stage. 1000 g of ore ground to a P80 of 200 μ was used in a laboratory Denver flotation cell. The tests were carried out at a pulp pH of 8.5, using Zn and Fe depressants ($ZnSO_4$ and NaCN), Pb-Cu collector (AR-3418) and frother (MIBC). Flotation is a separation technique based on differences in mineral surface properties. Adjusting the pH and using specific depressants allows the valuable minerals to be separated from the gangue efficiently [2].

Zinc sulfate ($ZnSO_4$) and sodium cyanide (NaCN) were selected as depressants for zinc and iron sulfides based on their proven effectiveness in minimizing zinc flotation in bulk Pb-Cu concentrate [19]. Similarly, the collector AR-3418 was chosen due to its selectivity for galena and chalcopyrite over sphalerite, as demonstrated in previous pilot studies. These

initial tests help to understand the behavior of the ore under different conditions, which is crucial to adjust the operating parameters and maximize the recovery of Pb and Cu while depressing Zn.

2.3 Standard Zn flotation

2.3.1 Zn mineral flotation

After the bulk Pb-Cu flotation stage, Zn mineral flotation was performed. Lime was added to adjust the pulp pH to 11, thus avoiding pyrite flotation. $CuSO_4$ was used as an activator and Xanthate Z-11 as a collector, together with MIBC as a frother. The test parameters were based on standard procedures used in the processing of sulfide minerals in the small-scale miners of the Oyón district. Adjusting the pH and adding specific activators and collectors is essential for selective zinc flotation. High pH suppresses pyrite flotation, while $CuSO_4$ activates sphalerite, and Xanthate Z-11 improves the hydrophobicity of zinc particles, facilitating their separation [10].

2.4 Evaluation of zinc displacement in bulk Pb-Cu flotation

2.4.1 Factorial experimental design

To monitor the displacement of Zn minerals during bulk Pb-Cu flotation, a 3-factor, 2-level, 2-replicate factorial experiment was designed using Minitab 19 statistical software. The factors evaluated were pulp alkalinity (pH), $ZnSO_4$ and NaCN dosage. 1000 g of ground sample at a P80 of 150 µ and a Denver flotation cell with 35% pulp solids were used. Factorial experimental designs allow the evaluation of the effect of multiple variables and their interactions on the flotation process, optimizing operating conditions to minimize zinc displacement in the Pb-Cu concentrate. The use of statistical software facilitates efficient and accurate analysis of the data obtained, providing a solid basis for decision making.

2.5 Experimental designs for zinc flotation

2.5.1 Zn flotation tests

Based on the best results of the Bulk Pb-Cu flotation, Zn flotation tests were developed to evaluate the contribution of the reagents Z-11 and MIBC. Factorial experimental designs of 2 factors, 2 levels and 2 replicas were used, developed in the Minitab 19 software. The evaluation of different reagents and their combinations through factorial designs allows to identify the optimal conditions for zinc flotation, improving the recovery and quality of the concentrate [3]. This approach ensures efficient optimization of process parameters, maximizing separation efficiency and reducing operating costs.

2.6 Zn recovery optimization

2.6.1 Optimization of flotation parameters

To optimize the flotation parameters, the response optimizer of the Minitab 19 statistical software was used. This process adjusts the operating conditions to maximize the recovery and quality of zinc in the concentrate. Optimization using statistical software identifies the best operating conditions, which allows maximizing the efficiency of the flotation process, reducing costs and improving the quality of the final product. This tool facilitates decisions based on quantitative data, increasing the reproducibility and reliability of the study.

3. RESULTS

3.1 Optical microscopy of the head mineral

Modal analysis of a representative sample of head ore was carried out at a granulometry of 75% - 200 mesh, using a polarizing light optical microscope, identifying copper species such as chalcopyrite with a distribution of 5.37%, and 97.27% release, Zn species such as sphalerite with a volume of 17.24%, and 99.51% free species, Pb species such as galena with a distribution of 7.41% and 97.73% free species, in addition traces of gold and electrum were observed, species considered to be of economic value, and are represented in Table 1.

Table 1. Species identified with optical microscopy

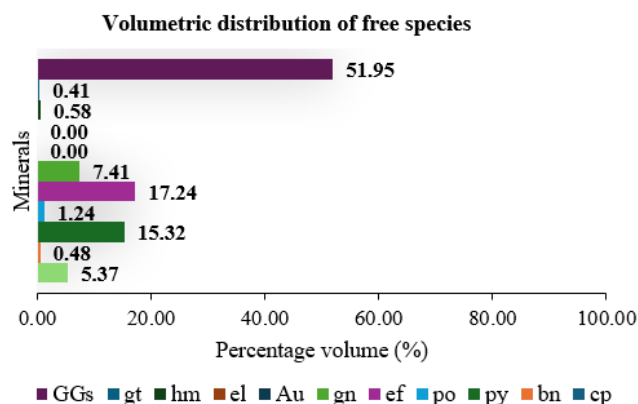| Minerals	Percentage Volume (%)	Release Rate (%)
Chalcopyrite	5.37	97.27
Bornite	0.48	78.26
Pyrite	15.32	98.08
Pyrrhotite	1.24	84.75
Sphalerite	17.24	99.51
Galena	7.41	97.73
Gold	Trazas	0.00
Electrum	Trazas	0.00
Hematite	0.58	82.14
Goethite	0.41	31.58
Gangas	51.95	98.67
Total	100.00	

Figure 1. Volumetric distribution of mineralogical species

Table 1 and Figure 1 show the volumetric distribution of the mineral species, which showed that gangues were found occupying a volume of 51.95%, a value that corresponds to just over half of the volume of the sample. In addition, iron sulfides such as pyrite and pyrrhotite could be observed with distributions of 15.32% and 1.24%, respectively.

The results from optical microscopy and TIMA electron microscopy show a strong consistency in identifying the main mineral species present in the ore, particularly with regards to sphalerite, chalcopyrite, and pyrite. Optical microscopy revealed a sphalerite distribution of 17.24% with 99.51% free species, which was closely matched by the TIMA analysis, where sphalerite/marmatite was recorded at 15.21% with 99.69% free species. Similarly, chalcopyrite was detected in both methods with a distribution of 5.37% (optical microscopy) and 4.98% (TIMA), reinforcing the reliability of these findings. However, the TIMA analysis provided additional insights into gangue mineral composition, identifying quartz (9.56%), muscovite (0.18%), and epidote (0.28%), which were either

not detected or less clearly differentiated by optical microscopy. This complementary relationship between both techniques enhances the overall understanding of the mineralogical composition, confirming that TIMA microscopy can offer a more detailed characterization of gangue minerals and their textural relationships, while optical microscopy provides essential information on the liberation and interlocking of economic minerals.

3.2 Interlocking of minerals

In the modal analysis, 5365 free particles and 98 entangled particles were counted, 18 entangled particles of gn-ef-py were observed, occupying a volume of 0.38%, and different types of entanglement, as shown in Table 1 and in the pie chart in Figure 1. Also, the main micrographs are represented in Figure 2 and Figure 3 as well as in Table 2.

Table 2. Distribution and release of entanglements

| Interlocking Minerals	Interlocking Type	Number of Particles	Distribution Percentage (%)	Chances of Complete Release
Free particles		5365	97.94	
py-po	1bIV	5	0.09	Moderately easy
	1aIII	9	0.21	Easy
	4aII	3	0.06	Very difficult
cp-bn	1bIV	4	0.07	Moderately easy
	1eIII	8	0.18	Very difficult to impossible
Au-GGs	1bIV	3	0.04	Moderately easy
	4bIII	6	0.15	Moderately difficult
	1aIII	4	0.07	Easy
gn-py-ef	1bIV	6	0.16	Moderately easy
	4aII	5	0.09	Very difficult
	2aII	3	0.06	Very difficult to impossible
el-gt-GGs	1bIV	3	0.06	Moderately easy
	1eIII	2	0.04	Very difficult to impossible
	4aII	5	0.10	Very difficult
	1eIII	8	0.18	Very difficult to impossible
	4bIII	4	0.08	Moderately difficult
	4aII	6	0.13	Very difficult
gt-hm-GGs	1eIII	3	0.06	Very difficult to impossible
	2bI	7	0.15	Very difficult
	1eIV	4	0.08	Very difficult to impossible
Total		**5463**	**100.00**	
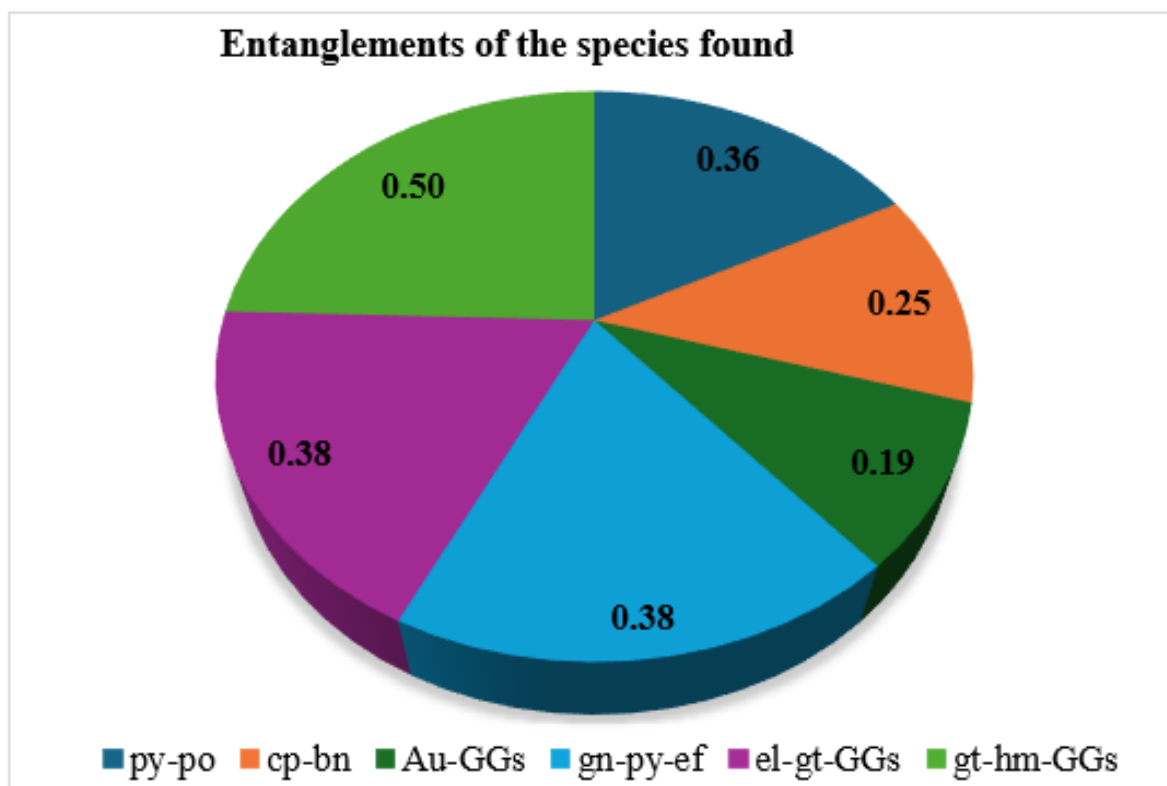
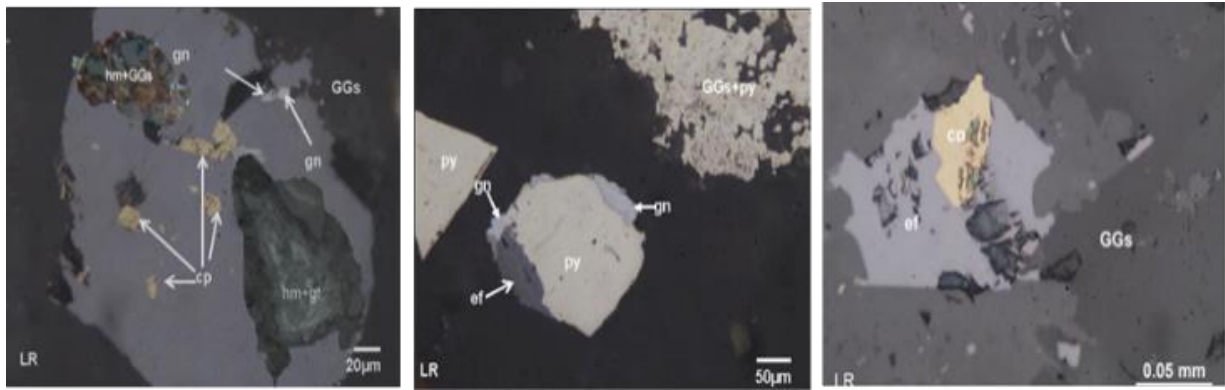**Figure 2.** Total distribution of interlaced species

Figure 3. Micrograph with presence of cp, gn, hm, gt and GGs (left), micrograph with presence of py, gn, ef and GGs (middle), micrograph with presence of cp, ef and GGs (right)

Table 3. Species identified with TIMA electron microscopy

Mineral	General Formula	Composition
Sphalerite/marmatite	$Zn_{0.825}Fe_{0.175}S$	15.21
Galena	PbS	6.02
Chalcopyrite	$CuFeS_2$	4.98
Bornite	Cu_5FeS_4	0.76
Pyrite/pyrrhotite	$FeS_2 / Fe_{1-x}S_x$	14.83
Other sulfides	-	0.58
Gold	Au	0.01
Electrum	-	0.02
Epidote	$(Ca_2)(Al_2Fe^{3+})(Si_2O_7)(SiO_4)O(OH)$	0.28
Garnet	$(Ca,Fe,Mg,Mn)_3(Al,Fe,Mn,Cr,Ti,V)_2(SiO_4)_3$	0.31
Quartz	SiO_2	9.56
Muscovite	$KAl_2(AlSi_3O_{10})(OH)_2$	0.18
Chlorite	$(Mg,Fe)_5Al(Si_3Al)O_{10}(OH)_8$	0.11
Biotite	$K(Mg,Fe)_3(AlSi_3O_{10}(OH,F)_2)$	0.08
Hematite	Fe_2O_3	0.45
Goethite	FeO_2H	0.26
Siderite	$FeCO_3$	0.02
Smithsonite	$ZnCO_3$	0.09
Cerussite	$PbCO_3$	0.12
Anglesite	$PbSO_4$	0.04
Rutile	TiO_2	0.12
Calcite	$CaCO_3$	0.26
Other	-	45.71
Total		100.00

3.3 Interlocking of minerals

A representative sample of polymetallic mineral was observed under the Tima electron microscope, in order to identify and classify the species of economic value and waste, by size, composition, and texture. Table 3 represents the total number of species identified by the electron microscope.

3.3.1 Zinc mineral species and their mineralogical ties

Table 4. Species identified with electron microscopy – Zn

Zn Ore	Composition (g)	Percentage Distribution (%)
Sphalerite / Marmatite	9.54	99.69
Smithsonite	0.03	0.31
Total	9.57	100.00

The largest contribution of Zn corresponded to marmatitic sphalerites with a distribution value of 99.69% of the total Zn species. In addition, oxidized Zn species such as Smithsonite could be identified, with a distribution of 0.31%, as observed in Table 4.

1. Degrees of liberation of marmatitic sphalerites

A liberation degree of 70.09% was determined for the marmatitic sphalerites, in addition, 25.77% was observed forming bonds and 4.41% was identified as occluded in another mineral species. Table 5 describes the analysis of the liberation degrees by size, and Figure 4 represents comparative bar graphs of the liberation degrees by size.
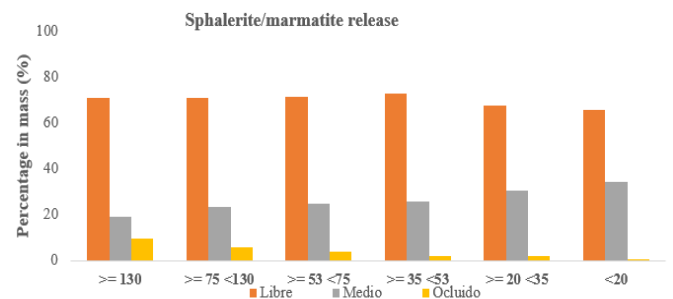

Figure 4. Representation of the percentage of liberation – sphalerite/marmatite

Table 5. Volumetric distribution according to its granulometry

Release of Sphalerite/Marmatite	Size [μm]						Total (%)
	>= 130	>= 75 <130	>= 53 <75	>= 35 <53	>= 20 <35	<20	
Free	71.16	70.78	71.55	72.69	67.78	65.59	70.09
Middle	19.10	23.49	24.69	25.55	30.37	34.41	25.77
Occluded	9.74	5.72	3.77	1.76	1.85	0.01	4.14
Total	**100.00**	**100.00**	**100.00**	**100.00**	**100.00**	**100.00**	**100.00**

2. Mineralogical assemblages of sphalerite

Sphalerite was observed forming groupings with pyrite, calcite and quartz, with distribution values of 5.32%, 9.60% and 4.28%, respectively. Other complex assemblages representing 2.05% of the sample volume were also identified, as shown in Table 6 and Figure 5.

Table 6. Zn mineral associations

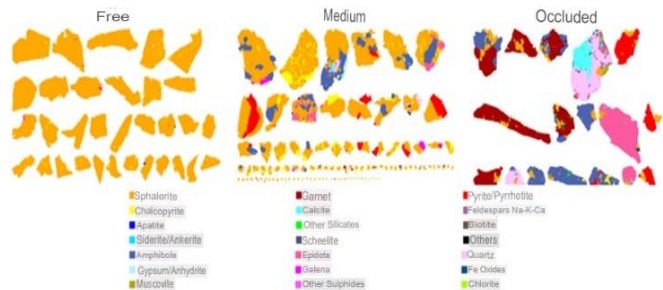| Zn Mineral Associations	Composition (g)	Percentage Distribution (%)
Sphalerite/marmatite	13.43	70.09
Sphalerite/marmatite: Pyrite	1.02	5.32
Sphalerite/marmatite: Calcite	1.84	9.60
Sphalerite/marmatite: Quartz	0.82	4.28
Other associations	2.05	10.70
Total	19.16	100.00

Figure 5. Particles according to their release - Zn

3.4 Chemical analysis of the head ore

A representative sample of the sulfide ore batch was assayed using volumetric methods to determine the grades of Pb, Zn and Cu, while for Au and Ag, the dry method was used. The results of the chemical analysis are described in Table 7.

Table 7. Zn mineral associations

Element	Pb (%)	Zn (%)	Cu (%)	Ag (Oz/TC)	Au (g/TM)
Worth	5.07	6.37	1.54	3.47	1.23

3.5 Standard flotation process

3.5.1 Standard bulk flotation of Pb-Cu

The beneficiation of polymetallic sulfide minerals in the province of Oyón is carried out through the flotation process in stockpile plants, which is carried out in a first stage of bulk flotation of Pb-Cu, depressing the Zn sulfides. The standard conditions of the first stage of bulk flotation of Pb-Cu are detailed in Table 8, and the metallurgical balance in Table 9 represents the results of the replication of the process at laboratory level, demonstrating a displacement of 13.53% of Zn, with a grade of 6.54% in the Pb-Cu bulk concentrate.

Table 8. Operating conditions of Pb-Cu flotation

Parameter	Worth
Weight	1200 g
pH	8.5
Granulometry	200 μ
$ZnSO_4$	120 g/TM
NaCN	40 g/TM
Depressor conditioning	5 min
AR-3418	30 g/TM
MIBC	15 g/TM
Collector conditioning	5 min
Floatation time	8 min

Table 9. Metallurgical balance of standard Pb-Cu flotation

Components	Weight	% Weight	Law					Metal					Recovery (%)					Ratio
			Pb (%)	Zn (%)	Cu (%)	Ag (Oz/TC)	Au (g/TM)	Pb	Zn	Cu	Ag	Au	Pb	Zn	Cu	Ag	Au	
Head	1200	100.00																
Bulk Pb-Cu	152.64	12.72	30.04	6.54	11.94	21.44	6.01	382.11	83.19	151.88	272.72	76.45	73.70	13.53	65.47	70.40	53.39	7.86
Medium Pb-Cu	301.47	25.12	3.67	1.56	2.57	1.1	0.43	92.20	39.19	64.56	27.63	10.80	17.78	6.38	27.83	7.13	7.54	
Tailings	745.89	62.16	0.71	7.92	0.25	1.4	0.9	44.13	492.29	15.54	87.02	55.94	8.51	80.09	6.70	22.46	39.07	
Head Calculated			5.18	6.14	2.32	3.87	1.43											

3.5.2 Standard Zn flotation

The tailings from the bulk Pb-Cu flotation were fed to the standard Zn flotation circuit, for which they were conditioned with $CuSO_4$ (5%) activating reagent at a pH of 11. The operating conditions for the standard Zn flotation are described in Table 10, and the results of the laboratory tests demonstrated a recovery of 96.35% of Zn with a quality of 42.74%, as represented in the metallurgical balance in Table 11.

3.6 Evaluation of zinc displacement in bulk Pb-Cu flotation

Based on the mineralogy, bulk Pb-Cu flotation tests were developed in order to evaluate the influence of the depressing reagents $ZnSO_4$ (5%) and NaCN (1%), in addition to the pH of the pulp, keeping the other operating variables constant (see Table 12), to minimize the displacement of Zn sulfides in the bulk Pb-Cu concentrate. Table 12 shows an experimental arrangement of 3 factors, two levels, and two replicas, whose

best test corresponds to the one of order N°7, reaching a recovery of 95.71% of Pb, 94.34% of Cu, and 79.29% of Ag. Likewise, a minimum displacement of zinc was achieved in the bulk concentrate, with a recovery value of 5.14% of Zn in the bulk, and a quality of 1.24%, for which 120 g/TM of $ZnSO_4$, 60 g/TM of NaCN were dosed, at a pH of 9.

The minimum and maximum values of the variables are described in Table 13. In addition, the factorial experimental design of metallurgical tests.

Table 10. Operating conditions of Zn flotation

Parameter	Worth
Weight	1000 g
pH	11
Granulometry	170 μ
$CuSO_4$	120 g/TM
Conditioning of depressant	10 minutos
Z-11	60 g/TM
MIBC	20 g/TM
Conditioning of collectors	5 minutos
Floatation time	10 minutos

3.6.1 Analysis of variance for zinc displacement in bulk Pb-Cu flotation

The ANOVA for the displacement of Zn in the bulk concentrate showed that the flotation pH was a determining factor in controlling the displacement, with a contribution

value of 72.59%, as well as $ZnSO_4$ and double and triple interactions being determining factors in controlling the displacement of zinc in the Pb-Cu bulk. The ANOVA results are shown in Figure 6, which represents the normal graph of standardized effects, and the level of significance of the variables studied, in controlling the displacement of Zn in the Pb-Cu concentrate.
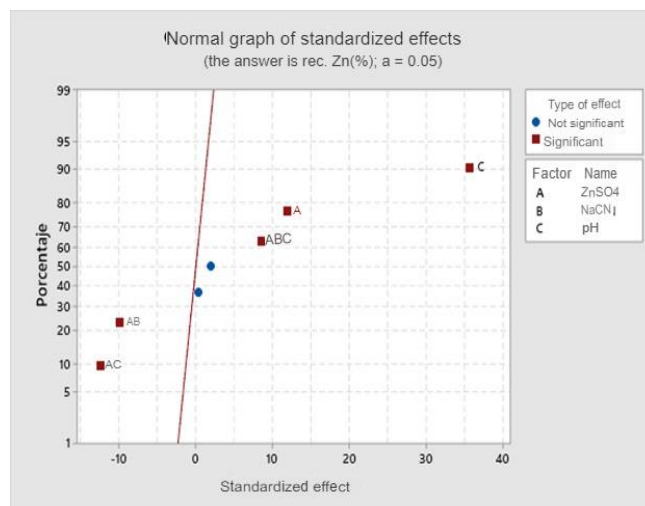

Figure 6. Standardized effects graph – Zn recovery in Pb-Cu bulk flotation

Table 11. Metallurgical balance of standard Zn flotation

Components	Weight	% Weight	Law					Metal					Recovery (%)					Ratio
			Pb (%)	Zn (%)	Cu (%)	Ag (Oz/TC)	Au (g/TM)	Pb	Zn	Cu	Ag	Au	Pb	Zn	Cu	Ag	Au	
Head	1000	100.00																
Bulk Pb-Cu	171.43	17.14	0.97	42.74	1.03	2.45	2.71	16.63	732.69	17.66	42.00	46.46	37.07	88.50	81.84	36.74	63.45	5.83
Medium Pb-Cu	224.89	22.49	0.45	2.89	0.04	0.8	0.17	10.12	64.99	0.90	17.99	3.82	22.56	7.85	4.17	15.74	5.22	
Tailings	603.68	60.37	0.3	0.5	0.05	0.9	0.38	18.11	30.18	3.02	54.33	22.94	40.37	3.65	13.99	47.52	31.33	
Head Calculated			0.44	8.27	0.21	1.14	0.73											

Table 12. 3-factor, 2-level, 2-replicate factorial design for bulk Pb-Cu flotation

Order Est	ZnSO$_4$	NaCN	pH	Rec. Pb(%)	Rec. Cu(%)	Rec. Zn(%)	Rec. Ag(%)	Rec. Au(%)
1	120	30	7	65.65	71.47	19.03	76.63	64.53
2	240	30	7	73.65	88.18	11.3	68.77	62.62
3	120	60	7	76.2	79.09	14.38	73.27	66.8
4	240	60	7	83.21	80.94	12.88	69.45	64.34
5	120	30	9	89.86	92.99	8.08	74.62	68.33
6	240	30	9	90.07	93.34	8.73	74.82	67.96
7	120	60	9	95.71	94.34	5.14	79.29	77.89
8	240	60	9	90.6	92.62	8.74	72.99	70.66
9	120	30	7	67.91	71.52	20.21	74.22	63.93
10	240	30	7	73.07	87.95	12.63	67.45	62.31
11	120	60	7	77.64	76.88	16.35	74.73	67.36
12	240	60	7	82.28	79.63	13.2	69.53	68.2
13	120	30	9	90.73	92.37	8.54	73.99	70.55
14	240	30	9	90.48	92.65	10.59	74.1	65.25
15	120	60	9	95.35	93.81	5.88	77.4	76.55
16	240	60	9	91.26	93.94	8.75	76.17	69.41

3.6.2 Experimental designs for zinc flotation

To evaluate the Zn flotation, the parameters of the bulk Pb-Cu flotation test No. 7 were taken into account, in order to prepare a representative sample to evaluate the recovery and quality of Zn, for which, the reagent dosage variables $CuSO_4$ (5%) and Z-11 (1%) were evaluated under the minimum and

maximum parameters, 150 to 300 for $CuSO_4$ (5%) and 40 to 80 for Z-11 (1%). Table 13 details the 2-level, 2-factor, and 2-replica factorial experimental design template, and their respective response variables, showing that the best results achieved a recovery of 97.61 of Zn with a quality of 48.06%, dosing 300 g/TM of $CuSO_4$ (5%), and 40 g/TM of Z-11 (1%).

Table 13. 2-factor, 2-level, 2-replicate factorial design for Zn flotation

Order Run	Pt Central	Blocks	CuSO₄	Z-11	Rec. Zn (%)	Law Zn (%)
1	1	1	150	40	85.35	37.74
2	1	1	300	40	97.22	47.13
3	1	1	150	80	92.75	40.17
4	1	1	300	80	93.19	43.13
5	1	1	150	40	85.23	38.09
6	1	1	300	40	97.61	48.06
7	1	1	150	80	92.57	39.94
8	1	1	300	80	92.95	38.02

1. Analysis of variance for zinc recovery

The analysis of variance for Zn recovery showed that the $CuSO_4$ dosage variable (5%) contributed 51.72%, and the interaction of the reagents used contributed 45.18% to the recovery variable. As a result of the analysis of the Zn recovery data, the model that predicts this response variable is presented, which presented a predictive correlation coefficient of 99.66%.

$$Rec.\ Zn(\%) = 54.082 + 0.15894(CuSO_4) + 0.4771(Z\text{-}11) - 0.001953(CuSO_4 * Z\text{-}11)$$

The charts in Figure 7 and Figure 8 graphically represent the standardized effects of the variables studied, with a reliability of 95%, which shows that the variables studied and their interactions are determining factors in determining the response variable.
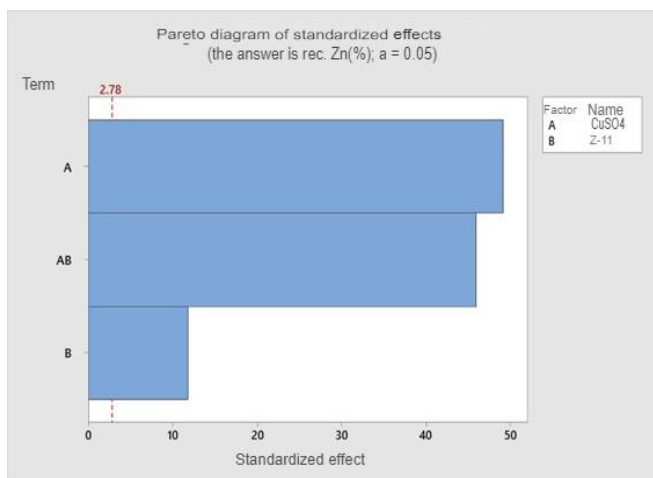

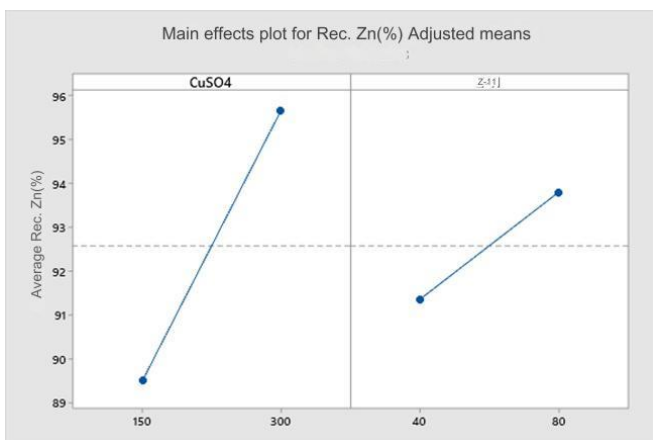**Figure 7.** Pareto chart of Zn recovery in Zn flotation

Figure 8. Main effects plot of Zn recovery in Zn flotation

2. Analysis of variance for zinc grade in concentrate

The ANOVA for the quality in the concentrate showed that the greatest contribution is made by the dosage of the reagent $CuSO_4$, with a value of 43.55%, as well as the interaction of the variables with a value of 35.12%. As a result of the analysis of variance, a mathematical model was presented, which predicts the quality of zinc in the flotation process, with a predictive correlation coefficient value of 54.54%. The regression equation:

$$Ley\ Zn(\%) = 16.94 + 0.1256(CuSO_4) + 0.282(Z\text{-}11) - 0.001527(CuSO_4 * Z\text{-}11)$$

The charts in Figure 9 and Figure 10 graphically represent the standardized effects of the variables studied, with a reliability of 95%, which demonstrates the greater contribution made by the dosage of copper sulphate, and the interaction of the variables studied, on the response variable.
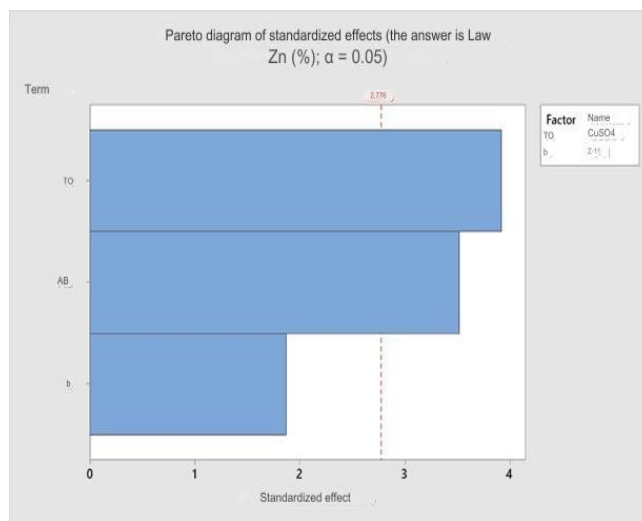

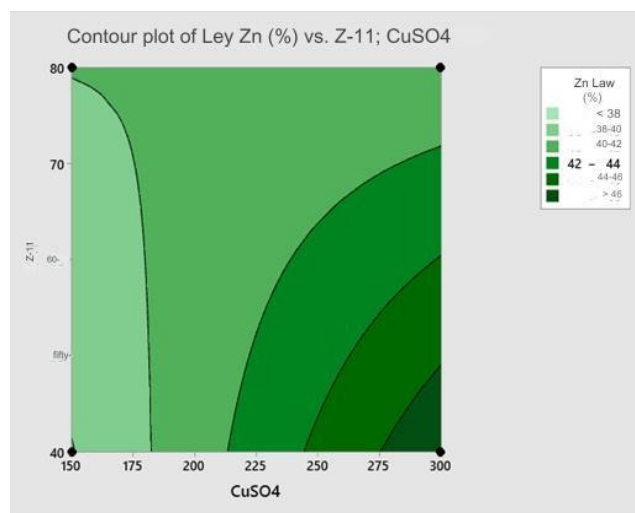**Figure 9.** Pareto chart of Zn law in Zn flotation

Figure 10. Contour plot of Zn law in Zn flotation

3. Zn recovery optimization

Using the statistical software Minitab 19, the independent variables were optimized to maximize the quality of Zn in the concentrate, as detailed in Table 14. The values of the optimized variables are presented in Figure 11.

Table 14. Adjustment of independent variables to maximize Zn recovery and grade

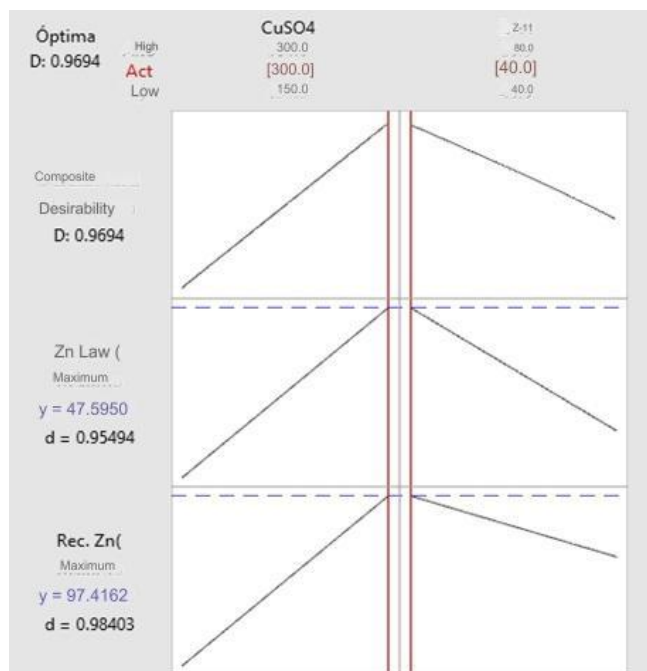| Solution	CuSO₄	Z-11	Law Zn (%) Adjustment	Rec. Zn(%) Adjustment	Compound Desirability
1	300	40	47.595	97.4162	0.969378

Figure 11. Optimization of Zn flotation

4. CONCLUSIONS

This research presents a novel approach by integrating advanced mineralogical characterization techniques, such as optical microscopy and TIMA, with a robust experimental design to optimize zinc recovery in sulfide ores under complex geometallurgical conditions. Unlike previous studies that focused on general flotation methods, this study addresses specific challenges related to mineralogical variability and interlocking species in the Oyón deposits. The findings demonstrate a significant improvement in zinc recovery (97.61%) and concentrate quality (48.06%), providing a replicable model for regions with similar geological complexities. This advancement contributes to filling critical gaps in knowledge about optimizing flotation processes for zinc sulfide ores.

The use of optical microscopy allowed for the identification of key mineral species and their textures, providing insights into the liberation and interlocking of economically valuable minerals. Complementarily, TIMA electron microscopy offered a more detailed characterization of gangue minerals, enhancing the understanding of their impact on the flotation process. The combination of these techniques, along with a comprehensive experimental design, was crucial in identifying the optimal conditions for zinc recovery, including reagent dosages and pH levels. This methodological approach enabled a precise analysis of the mineralogical complexity of the Oyón deposits, leading to more efficient processing strategies.

Optical microscopy and TIMA electron microscopy of representative samples of polymetallic sulfide ore allowed the identification of various mineral species. Marmatitic sphalerites represented a volumetric distribution of 17.24% (optical microscopy) and 15.21% (electron microscopy), with 99.51% of free species observed optically. Copper species such as chalcopyrite and bornite were also identified, with distributions of 5.37% and 0.48%, respectively, as well as galena (7.41%) and traces of gold and electrum. Electron microscopy additionally identified oxides such as smithsonite (0.09%) and gangues such as quartz (9.56%).

The most influential variable to minimize Zn displacement in bulk Pb-Cu flotation was pulp pH, with a contribution value of 72.59%. The flotation tests with the best conditions achieved minimum Zn displacement values of 5.14% and 5.88%, using 60 g/MT of NaCN, 120 g/MT of ZnSO₄ and a pH of 9. The double interactions ZnSO₄NaCN and ZnSO₄pH also showed significant contributions of 5.64% and 8.92%, respectively.

In the Zn flotation stage, the best tests achieved recoveries of 97.22% and 97.61%, with grades of 48.06%, using 300 g/MT of CuSO₄ and 40 g/MT of Z-11. The analysis of variance indicated that the variable CuSO₄ was decisive for the Zn recovery, with a contribution of 43.55%, while the interaction CuSO₄ - Z-11 contributed with 35.12%. The predictive model for Zn recovery showed a correlation coefficient of 99.66%.

Optimization of reagent consumption indicated that using 300 g/MT of CuSO₄ and 40 g/MT of Z-11 resulted in a recovery of 97.41% and a grade of 47.60% of Zn, validating the values calculated by the variable optimizer of the Minitab-19 software. The findings of this study have significant implications for industrial flotation practices, particularly in mining operations where zinc sulfide ores are prevalent. The optimized flotation conditions identified in this research, such as precise control of pH and reagent dosage, can be applied to improve the recovery and quality of zinc concentrates in other mining operations facing similar mineralogical challenges. Additionally, the use of advanced mineralogical characterization techniques could be adopted by industry to enhance the efficiency of their flotation processes, reducing operational costs and improving sustainability. These results highlight the importance of adjusting operating conditions and reagent doses to maximize the efficiency and quality of the Zn concentrate.

REFERENCES

[1] El-Omairi, M.A., El Garouani, A. (2023). A review on advancements in lithological mapping utilizing machine learning algorithms and remote sensing data. Heliyon, 9(9): e20168. https://doi.org/10.1016/j.heliyon.2023.e20168

[2] Gonzalez-Alvarez, I., Goncalves, M.A., Carranza, E.J.M. (2020). Introduction to the special issue challenges for mineral exploration in the 21st century: Targeting mineral deposits under cover. Ore Geology Reviews, 126: 103785. https://doi.org/10.1016/J.OREGEOREV.2020.103785

[3] Rostek, L., Pirard, E., Loibl, A. (2023). The future availability of zinc: Potential contributions from recycling and necessary ones from mining. Resources, Conservation & Recycling Advances, 19: 200166. https://doi.org/10.1016/J.RCRADV.2023.200166

[4] Backman, C.M. (2008). Global supply and demand of metals in the future. Journal of Toxicology and

Environmental Health, Part A, 71(18): 1244-1253. https://doi.org/10.1080/15287390802209582

[5] Gao, R., Folens, K., Mees, B., Du Laing, G., Rabaey, K., Bonin, L. (2021). Copper and zinc extraction from automobile shredder residues via an integrated electrodeposition and crystallization process. Resources, Conservation and Recycling, 172: 105672. https://doi.org/10.1016/J.RESCONREC.2021.105672

[6] Kwon, G., Yoon, K., Kwon, E., Park, J., Lee, H., Song, H. (2024). Technical advancement in valorization of electronic waste and its contribution to establishing economic value-chain. Chemical Engineering Journal, 494: 153154. https://doi.org/10.1016/j.cej.2024.153154

[7] Jia, L., Zhong, Y., Li, K., Li, B., Gao, J., Liu, T., Wang, F., Wu, W., Feng, J. (2023). Recovery of zinc resources from secondary zinc oxide via composite ammonia leaching: Analysis of Zn leaching behavior. Chemical Engineering Journal, 472: 144930. https://doi.org/10.1016/j.cej.2023.144930

[8] Jha, M.K., Kumar, V., Singh, R.J. (2001). Review of hydrometallurgical recovery of zinc from industrial wastes. Resources, Conservation and Recycling, 33(1): 1-22. https://doi.org/10.1016/S0921-3449(00)00095-1

[9] Hasan, M.A., Hossain, R., Sahajwalla, V. (2023). Critical metals (Lithium and Zinc) recovery from battery waste, ores, brine, and steel dust: A review. Process Safety and Environmental Protection, 178: 976-994. https://doi.org/10.1016/J.PSEP.2023.08.069

[10] Deng, X., Huang, R., Lv, X., Yang, J., Yang, J. (2022). Separation and recovery of metallic zinc and iron concentrate from blast furnace dust by vacuum carbothermal reduction. Process Safety and Environmental Protection, 162: 746-751. https://doi.org/10.1016/j.psep.2022.04.050

[11] Kaksonen, A.H., Deng, X., Bohu, T., Zea, L., Khaleque, H.N., Gumulya, Y., Boxall, N.J., Morris, C., Cheng, K.Y. (2020). Prospective directions for biohydrometallurgy. Hydrometallurgy, 195: 105376. https://doi.org/10.1016/J.HYDROMET.2020.105376

[12] Potysz, A., Pędziwiatr, A., Hedwig, S., Lenz, M. (2020). Bioleaching and toxicity of metallurgical wastes. Journal of Environmental Chemical Engineering, 8(6): 104450. https://doi.org/10.1016/J.JECE.2020.104450

[13] Chandra, A.P., Gerson, A.R. (2010). The mechanisms of pyrite oxidation and leaching: A fundamental perspective. Surface Science Reports, 65(9): 293-315. https://doi.org/10.1016/J.SURFREP.2010.08.003

[14] Chen, W., Dai, Y., Liu, Z., Zhang, H. (2024). The evolution of global zinc trade network: Patterns and implications. Resources Policy, 90: 104727. https://doi.org/10.1016/J.RESOURPOL.2024.104727

[15] Jia, K., Jin, Y., Liu, S., Qin, W., Zhang, C., Li, G., Cao, Y. (2024). The application and mechanism of degradable activator biologically small molecule organic acids in smithsonite flotation. Applied Surface Science, 660: 159907. https://doi.org/10.1016/j.apsusc.2024.159907

[16] Lu, M., Zhao, Y. (2024). Mineral resource extraction and environmental sustainability for green recovery. Resources Policy, 90: 104616. https://doi.org/10.1016/j.resourpol.2023.104616

[17] Chávez, C.A.R., Layme, M.Q., Layme, W.Q., Pinto, S.L.A., Palma, Y.M.P., Sonco, V.Y.F.M. (2023). Relación de la producción minera con la actividad agrícola y pecuaria en la región Puno, Perú. Revista Alfa, 7(19): 193-208. https://doi.org/10.33996/REVISTAALFA.V7I19.209

[18] Chen, Y., Sun, Y., Han, Y. (2024). Efficient flotation separation of lead–zinc oxide ores using mineral sulfidation reconstruction technology: A review. Green and Smart Mining Engineering, 1(2): 175-189. https://doi.org/10.1016/J.GSME.2024.05.004

[19] Tian, C., Tang, Z., Zhang, H., Xie, Y., Dai, Z. (2024). Reagent dosage inference based on graph convolutional memory perception network for zinc roughing flotation. Control Engineering Practice, 146: 105882. https://doi.org/10.1016/J.CONENGPRAC.2024.105882

[20] Wu, Z., Xiong, Z., Lai, B. (2022). Metal sulfide-based catalysts in advanced oxidation processes for water decontamination. Environmental Functional Materials, 1(3): 298-315. https://doi.org/10.1016/J.EFMAT.2023.01.004

[21] Clarke, P., Fornasiero, D., Ralston, J., Smart, R.S.C. (1995). A study of the removal of oxidation products from sulfide mineral surfaces. Minerals Engineering, 8(11): 1347-1357. https://doi.org/10.1016/0892-6875(95)00101-U

[22] Dominy, S.C., O'Connor, L., Parbhakar-Fox, A., Glass, H.J., Purevgerel, S. (2018). Geometallurgy—A route to more resilient mine operations. Minerals, 8(12): 560. https://doi.org/10.3390/MIN8120560

[23] Tiu, G., Ghorbani, Y., Jansson, N., Wanhainen, C., Bolin, N.J. (2023). Quantifying the variability of a complex ore using geometallurgical domains. Minerals Engineering, 203: 108323. https://doi.org/10.1016/j.mineng.2023.108323

NOMENCLATURE

ZnSO$_4$	Zinc Sulfate
NaCN	Sodium Cyanide
CuSO$_4$	Copper Sulfate
P80	Particle size below which 80% of the material is found
Xanthate Z-11	Xanthate used as collector in the flotation process
pH	A measure of acidity or alkalinity of a solution